Supporting Information

Stabilization of All-Solid-State Li-S Batteries with a Polymer-Ceramic Sandwich Electrolyte by Atomic Layer Deposition

Jianneng Liang[a], Qian Sun[a], Yang Zhao[a], Yipeng Sun[a], Changhong Wang[a], Weihan Li[a], Minsi Li[b], Dawei Wang[a], Xia Li[a], Yulong Liu[a], Keegan Adair[a], Ruying Li[a], Li Zhang[c], Rong Yang[c], Shigang Lu[c], Henry Huang[d], Xueliang Sun[a]*

[a.] *Department of Mechanical and Materials Engineering, University of Western Ontario, London, ON. N6A 5B9, Canada*

[b.] *Department of Chemistry, University of Western Ontario, London, ON. N6A 5B7, Canada*

[c.] *China Automotive Battery Research Institute Co., Ltd., 5th Floor, No. 43, Mining Building, North Sanhuan Middle Road, Haidian District, Beijing 100088, China*

[d.] *Glabat Solid-State Battery Inc. 700 Collip Circle, Suite 211, London, ON, N6G 4X8, Canada*

Corresponding Author

*Xueliang Sun. E-mail: xsun@eng.uwo.ca

Supporting Figures (and Corresponding Discussions)

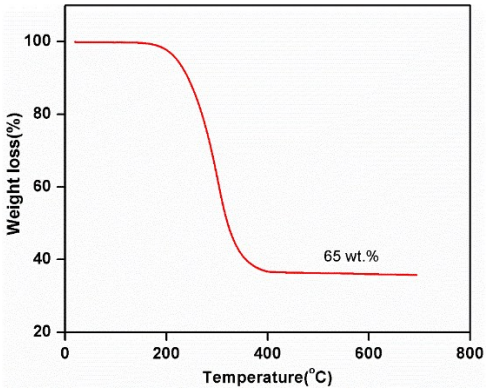

Figure S1. TGA analysis of C-S composite

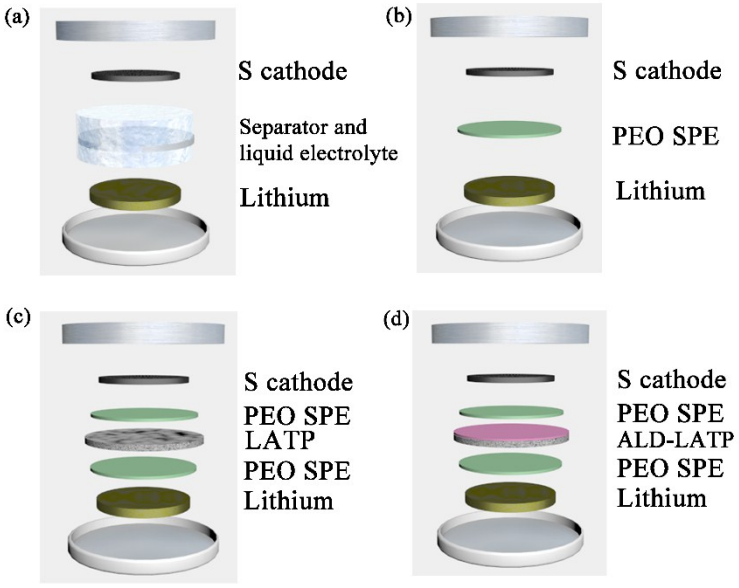

Figure S2. Schematic diagram shows the configurations of Li-S batteries in our studies. (a) Liquid-based Li-S battery; (b) All-solid-state Li-S battery with PEO SPE; (c) All-solid-state Li-S battery with PLP SSE; (d) All-solid-state Li-S battery with ALD-PLP SSE

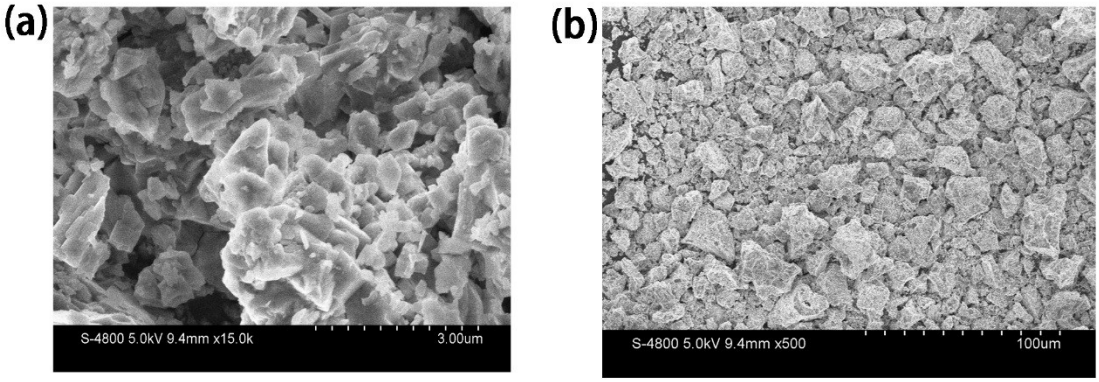

Figure S3. SEM images of LATP precursor after calcinating at 700 ^{o}C for 2 h. (a) high magnification, (b) low magnification.

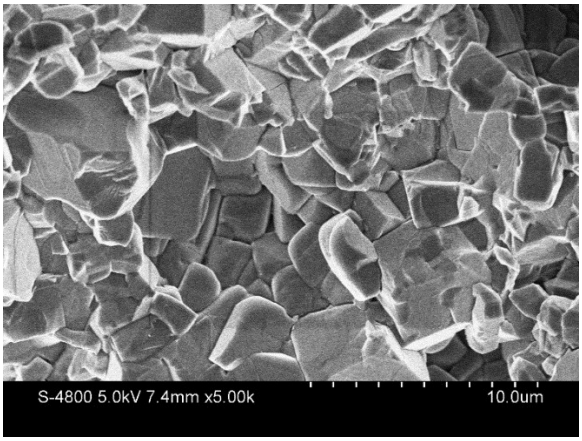

Figure S4. Cross section SEM image of LATP SSE after sintering at 900 ^{o}C, 6 h.

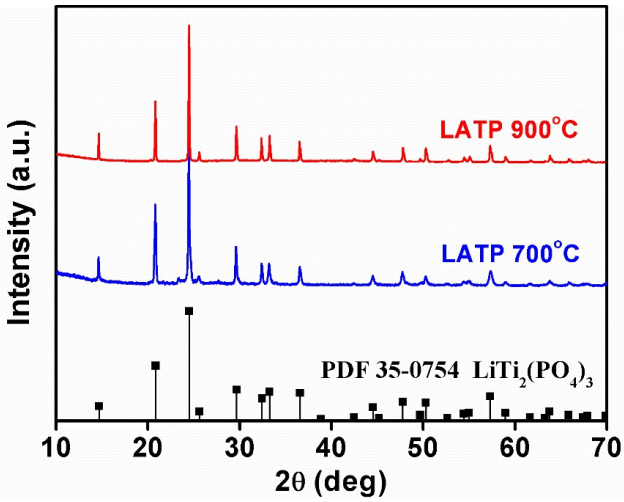

Figure S5. XRD patterns of LATP after calcinating at 700 °C and after sintering at 900 °C.

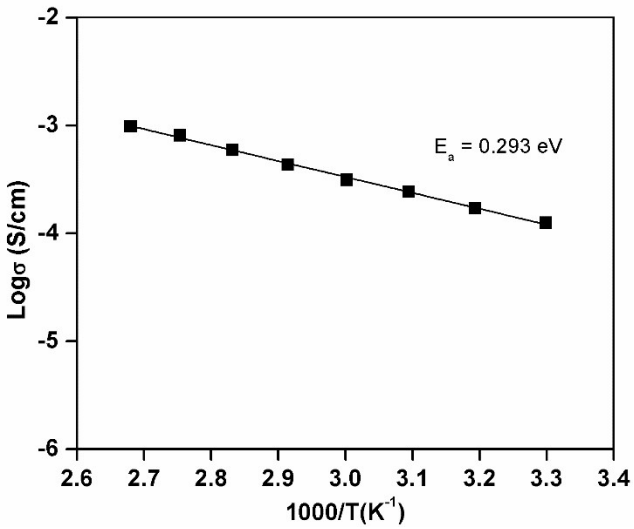

Figure S6. Temperature dependent ionic conductivity of LATP SSE after sintering at 900 °C.

NASICON-type LATP was prepared by a solid-state reaction method described in our previous work.[1] LATP pellets were polished to a thickness of around 500 µm before ALD Al_2O_3 coating process. The morphology of LATP after calcination are presented in Figure S3a, b. The particle size of the LATP precursor is around 200-500 nm with secondary aggregates ranging from 10 to 50 µm in dimension (Figure S3b). After sintering at 900 °C, LATP particles are well bonded to each other and a dense structure can be obtained (Figure S4). Both LATP powder and LATP pellet are found to exhibit the same phase as parent crystal structure $LiTi_2(PO_4)_3$ (PDF 35-0754) phase structure (Figure S5). The ionic conductivity

of LATP is 1.6*10^{-4} S/cm at RT with an activation energy (Ea) of 0.293 eV (Figure S6), which is consistent with previously reported results.[1, 2]

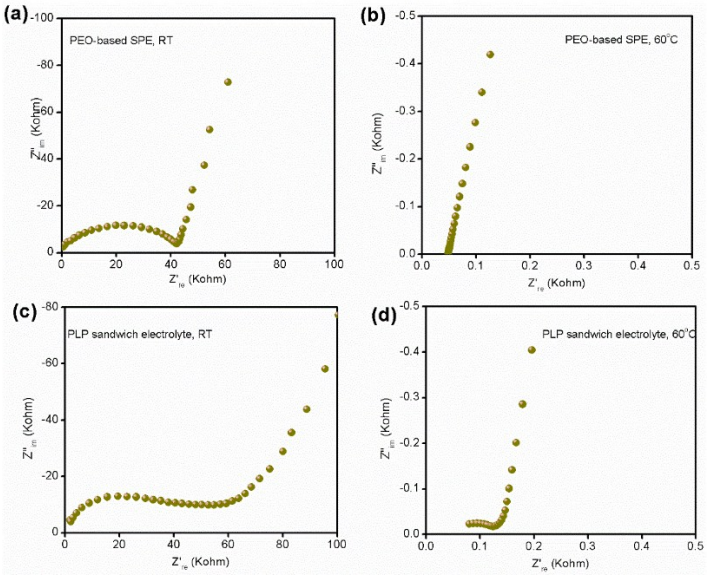

Figure S7. EIS of (a) PEO-based SPE at RT, (b) PEO-based SPE at 60 °C, (c) PLP sandwich-type hybrid electrolyte at RT and (d) 60 °C.

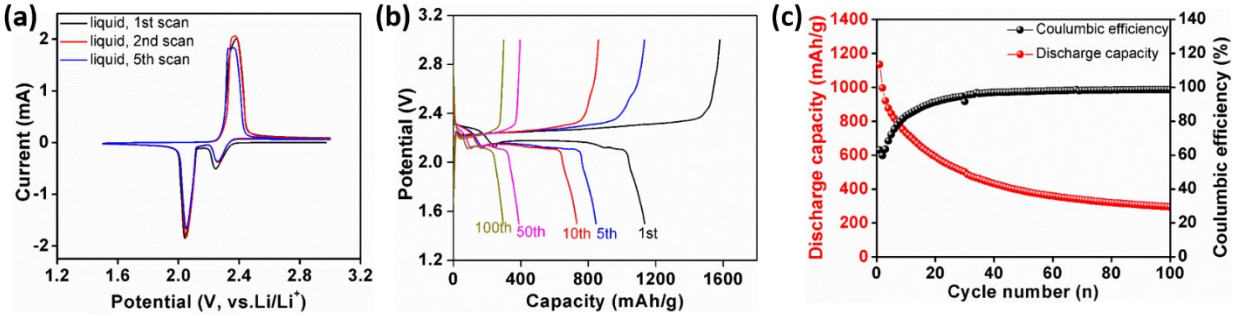

Figure S8. (a) CV cure of liquid-based Li-S battery, (b) charge/discharge profile of liquid-based Li-S battery, (c) discharge capacity and coulombic efficiency of liquid-based Li-S battery. All testing is performed at 60 °C.

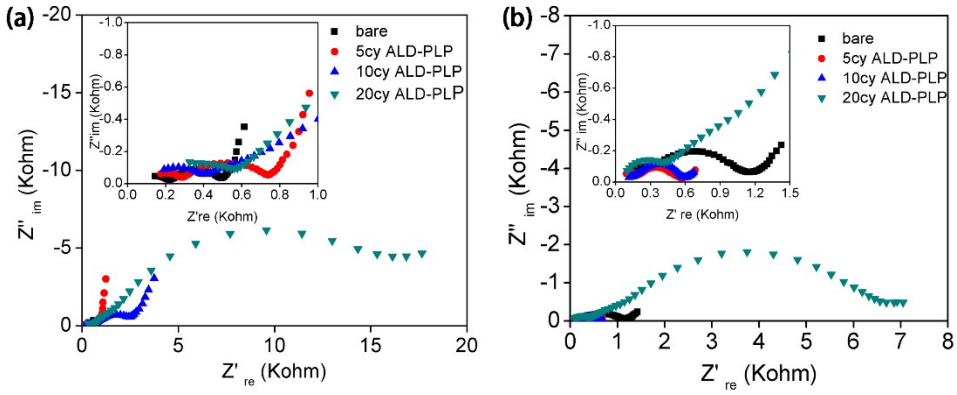

Figure S9. EIS of ASSLSBs with different cycles ALD coating PLP sandwich-type hybrid electrolyte at 60 °C (a) before charge/discharge testing and (b) after 100 charge/discharge cycles.

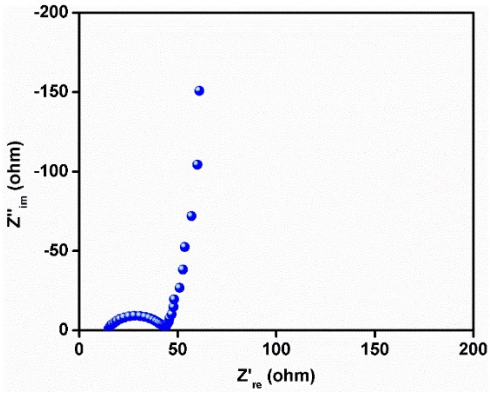

Figure S10. EIS of Liquid-based Li-S battery at 60 °C before charge/discharge testing. The overall impedance of liquid-based Li-S battery is 44 Ω, much smaller than that of ASSLSBs with PLP electrolyte (~500 Ω).

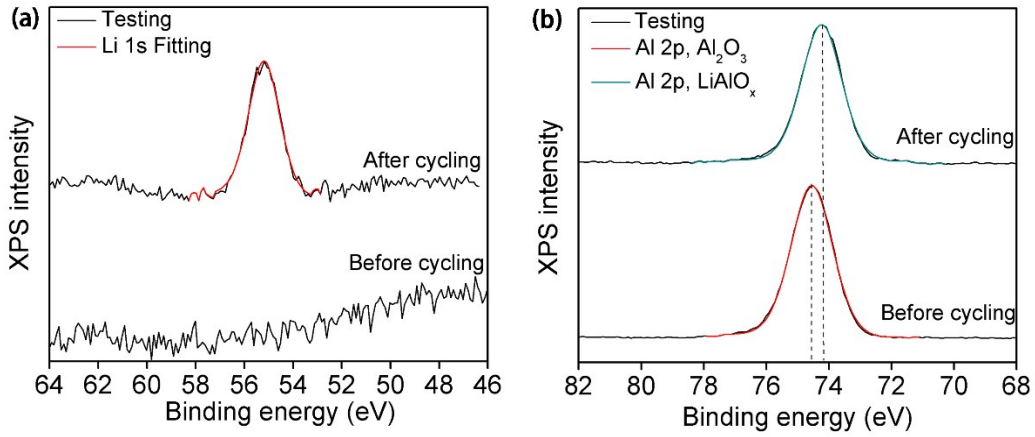

Figure S11 Comparisons of Li 1s and Al 2p XPS on 50cy ALD coating LATP surface before charge/discharge and after 10 cycles charge/discharge.

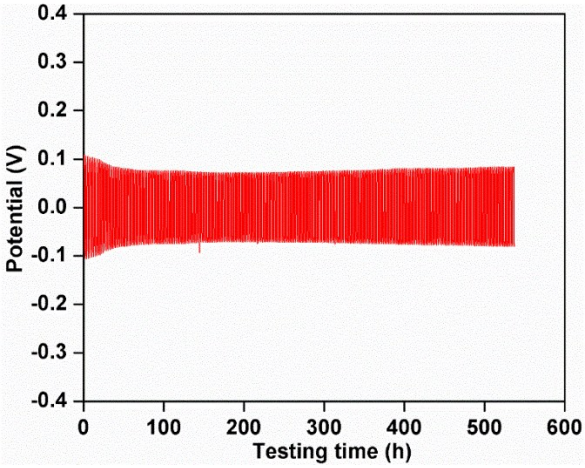

Figure S12. Potential profile of lithium symmetric cell with PLP SSE at 60 °C, current density 0.1 mA/cm^2, with a cut-off capacity 0.1 mAh/cm^2.

The LATP SSE is known to suffer from chemical instability against the lithium metal anode where the Ti^{4+} is reduced. However, SPEs can be applied between the LATP SSE and lithium anode, leading to the formation of a stable interface that can inhibit dendrite growth[3]. Figure S12 shows the lithium plating/stripping process of lithium symmetric cell with PLP sandwich-type hybrid electrolyte at a current density of 0.1 mA/cm^2. Over 500 h testing period, no short circuit or overpotential growth could be observed, which indicates a stable plating/stripping process with no dendrite formation.

The symmetric cell observation is consistent with previous reports.[3] This result eliminates the possibility of the reduction of LATP in ASSLSBs by lithium anode.

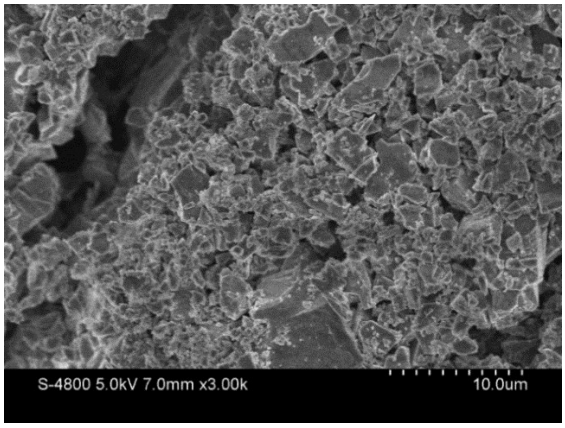

Figure S13. Bare LATP after 100 charge/discharge cycles in ASSLSB. The formation of the small particles indicates the decomposition of LATP by polysulfide.

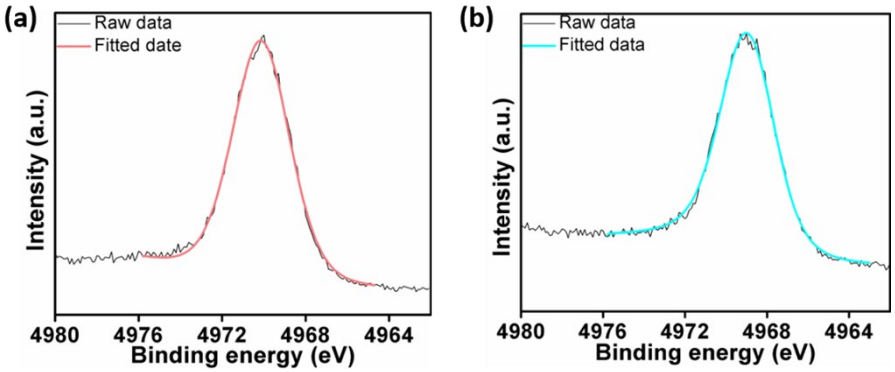

Figure S14. (a) Ti 1s XPS of pristine LATP and (b) Ti 1s XPS of reduced-LATP by polysulfide solution.

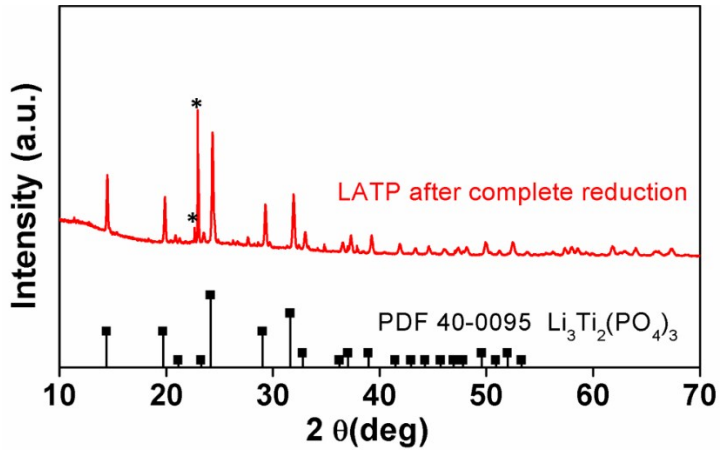

Figure S15. XRD of completely reduced-LATP. (* sulfur) The existence of sulfur peaks is due to the oxidation of Li_2S_6 by LATP.

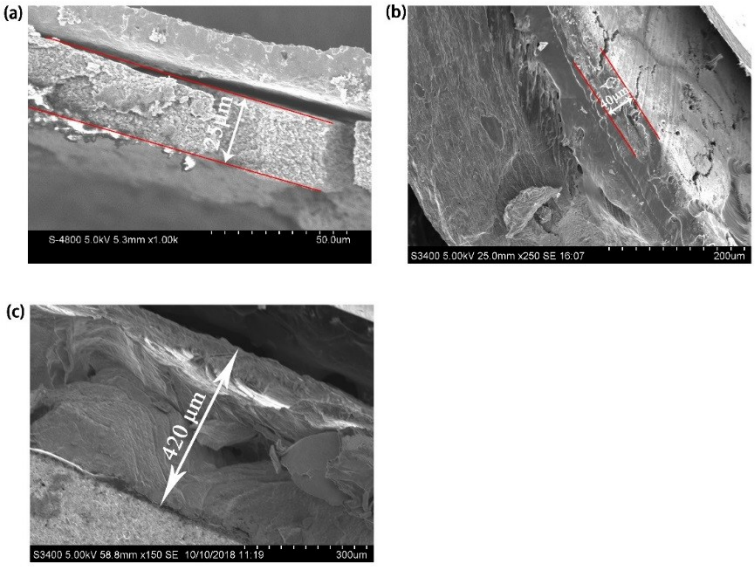

Figure S16 Cross-section SEM images of (a) C-S cathode; (b) C-S cathode after 100 cycles charge/discharge. (c) Lithium anode after 100 cycles charge/discharge.

Figure S16(a) is the cross-section SEM image of a C-S cathode with current collector. The thickness of the cathode layer is 25 μm. After the cathode was charge/discharge for 100 times, the thickness of the cathode is 40 μm. The volume expansion is 60 % which is significant large. For the anode part, the SEM image of lithium anode after 100 cycles was obtained, whose thickness is 420 μm. 10 μm thicker than the original lithium anode (410 μm).

Table S1. A comparison of the all-solid-state Li-S batteries performances

Solid-state electrolyte	Sulfur loading (mg/cm^2)	Initial capacity (mAh/g)	Cycling performance (mAh/g)	Refs.
PEO-$LiCF_3SO_3$	/	520 (0.05C)	300 (Second cycles, 0.05C)	4
PEO-PEGDA-DVB cross-linking polymer-LITFSI	/	375 (0.05C)	175 (50^{th} cycles, 0.05C)	5
Polyether-based polymer-$LiClO_4$-SiO_2	0.34	1131	About 965 (first charge)	6
Sucrose-boron polymer-PEO-LITFSI	About 0.8 (PAN-S)	1302 (0.1C)	About 620 (100^{th} cycles, 0.1C)	7
PEO-LITFSI	/	900 (0.05C)	About 700(50^{th} cycles, 0.05C)	8
PEO-$LiCF_3SO_3$-ZrO_2	/	About 170	About 172 (50^{th} cycles)	9
PEO-LiTFSI-SiO_2	/	1265	800 (25^{th} cycles)	10
PEO-LiTFSI-$LiAlO_2$		609	280 (10^{th} cycles)	11
PEO/ALD-LATP/PEO	0.6~1	1035 (0.1C)	823 (100^{th} cycles, 0.1C)	**This work**

Table S2. XPS fitting results

Sample name	Bare LATP	5 ALD-LATP	10 ALD-LATP	20ALD-LATP
Content of Ti^{4+} (%)	28.7	56.8	62.6	70.8
Content of reduced-Ti (%)	71.3	43.2	37.4	29.2

References

1. C. Wang, Q. Sun, Y. Liu, Y. Zhao, X. Li, X. Lin, M. N. Banis, M. Li, W. Li, K. R. Adair, D. Wang, J. Liang, R. Li, L. Zhang, R. Yang, S. Lu and X. Sun, Nano Energy, 2018, 48, 35-43.
2. J. Liu, T. Liu, Y. Pu, M. Guan, Z. Tang, F. Ding, Z. Xu and Y. Li, RSC Advances, 2017, 7, 46545-46552.
3. W. Zhou, S. Wang, Y. Li, S. Xin, A. Manthiram and J. B. Goodenough, Journal of the American Chemical Society, 2016, 138, 9385-9388.
4. L. Carbone and J. Hassoun, Ionics, 2016, 22, 2341-2346.
5. O. Garcia-Calvo, N. Lago, S. Devaraj and M. Armand, Electrochimica Acta, 2016, 220, 587-594.
6. H. Marceau, C.-S. Kim, A. Paolella, S. Ladouceur, M. Lagacé, M. Chaker, A. Vijh, A. Guerfi, C. M. Julien and A. Mauger, Journal of Power Sources, 2016, 319, 247-254.
7. K. Liu, Y. Lin, J. D. Miller, J. Liu and X. Wang, J Electrochem Soc, 2017, 164, A447-A452.
8. X. Judez, H. Zhang, C. Li, J. A. González-Marcos, Z. Zhou, M. Armand and L. M. Rodriguez-Martinez, The Journal of Physical Chemistry Letters, 2017, 8, 1956-1960.
9. J. Hassoun and B. Scrosati, Advanced Materials, 2010, 22, 5198-5201.
10. X. Liang, Z. Wen, Y. Liu, H. Zhang, L. Huang and J. Jin, Journal of Power Sources, 2011, 196, 3655-3658.
11. X. Zhu, Z. Wen, Z. Gu and Z. Lin, Journal of Power Sources, 2005, 139, 269-273.